Iranian Journal of Organic Chemistry Vol. 13, No. 2 (2021) 3075-3091

CdO/ZnO supported silver nanoparticles as a reusable heterogeneous catalyst for one-pot synthesis of new pyrrolobenzoazepines

Annataj Noushin[a], Ali Varasteh-Moradi[a], S. Zahra Sayyed-Alangi[*b], Zinatossadat Hossaini[c], Sattar Arshadi[d]

[a]*Department of Chemistry, Gorgan Branch, Islamic Azad University, Gorgan, Iran*
[b]*Department of Chemistry, Azadshahr Branch, Islamic Azad University, Azadshahr, Iran*
[c]*Department of Chemistry, Qaemshahr Branch, Islamic Azad University, Qaemshahr, Iran*
[d]*Department of Chemistry, Payam Noor University, Behshahr, Iran*

Received: February 2021; Revised: March 2021; Accepted: March 2021

Abstract: In this study, a new, economical, environment-friendly, and green method was reported for the synthesis a family of substituted pyrrolobenzoazepines using the one-pot condensation reactions of isatin, ammonium acetate, α-haloketones, and activated acetylenic compounds in water at room temperature in the presence Ag/CdO/ZnO nanocomposites (Ag/CdO/ZnO NCs) as a new heterogeneous catalyst. For confirming the structure of synthesized nanocatalyst, uv, XRD, FESEM, and EDX analyses were utilized. Another subject in this research is an evaluation of the antioxidant power of some synthesized pyrrolobenzodiazepines by diphenyl-picrylhydrazine (DPPH) radical trapping experiment. The short time of reaction, high yields of product, simple removing of catalyst and products are some benefits of this process.

Keywords: Ag/CdO/ZnO NCs, pyrrolobenzoazepines, Green synthesis.

Introduction

Heterocyclic compounds hold a prominent position in medicinal chemistry owing to their wide spectrum of biological activities such as antimalarial,[1] antimicrobial,[2] antitumor,[3] anticancer, [4] antidepressant,[5] antiviral,[6] antidiabetic,[7] anti-inflammatory [8] and anti-HIV. [9] Moreover, they also contribute to the field of material science, [10] dyes and pigment science [11] as well as agrochemistry. [12] Therefore, there is considerable thrust for the development of efficient synthetic strategies for producing these compounds. MCRs open diverse avenues to create novel concatenations in one-pot fashion leading to diverse biologically potent heterocyclic scaffolds. [13, 14] Having a case ade of reactions occurring in one pot is highly beneficial in the context of modern trends for organic c synthesis, where sustainability is as relevant as efficiency and selectivity.

Multicomponent reactions being atom economic, efficient ,and extremely convergent in nature offer a number of advantages over stepwise sequential approaches [15–17] and could be performed in the presence of nanocatalyst and produce heterocyclic compounds.[18-20] Among the heterocyclic compounds, pyrrolobenzodiazepines (PBDs) are a family of naturally occurring antitumor antibiotics, [21] and completely synthetic PBD dimmers have been developed that crosslink DNA in a sequence-selective fashion, leading to cell cycle arrest (G2/M boundary) and apoptosis at picomolar concentrations of the drug. [22, 23] Transition metal oxides nanostructures due to their unique features such as high specific surface area, chemical stability and electrochemical activity at the nanoscale with promising applications in applied science and technology[24-26] have been broadly utilized. bimetallic or trimetallic mixed oxide catalysts, in particular, have attracted significant attention, in the recent past due their wonderful capabilities to perform organic reactions with high selectivity and

*Corresponding author: Email: zalangi@iauaz.ac.ir Fax:+981142142537; Tel.:+981142142505

efficiency[27-29] Metal oxides are highly crystalline for their catalytic efficacy [30, 31] and the combination of two or more metals and their curing processes allow the tuning of the surface properties of the materials, making them opt for a specific purpose [32, 33] Thus, mixed oxide catalysts and their nanocomposites offer wide range of advantages including atom efficiency and green principles [34, 35] The surface properties such as charged/adsorbed entities, [36] acidic and basic characteristics, [37, 38] tendency of cations to undergo redox reactions, [39] and oxygen vacancies all contribute to their catalytic activity. [40] Many catalytic procedures established using such mixed oxide catalysts are simple preparation,[41] efficient and environmentally friendly. These are applied both for their acidic and basic possessions,[42] and their reduction-oxidation properties which make them a vital class in heterogeneous catalysis. Mixed oxide catalysts address sustainability concerns and provide alternative and efficient methods for various important organic transformation reactions.[43-45] Many novel mixed oxide catalysts with superb activity, excellent chemical and thermal stability, high surface area, low-cost and recyclability have been reported with precise applications in synthetic organic chemistry.[46-50] Their heterogeneous nature facilitates easy separation from the reactants and products, making them attractive for reusability.[51, 52] Generally various physical and chemical methods are applied to the synthesis of catalysts [53-57] Many efforts have been done to develop green methods for the synthesis of NPs to remove the disadvantages of previous methods. The biosynthetic technique for the synthesis of nanocatalyst using plant extracts is a good alternative method. This green method is safe, simple, eco-friendly and cost-effective.[58] Another topic in this research work is the evaluation of antioxidant activity in some of synthesized pyrrolobenzoazepines derivatives. Usually the compounds that because of reductive property and chemical structure of them could be reduced or deleted negative effect of free radicals have antioxidant properties. Many diseases such as cardiovascular, inflammatory bowel syndrome, cancer, aging, and Alzheimer.[59-61] could be prevented or decrease with compounds with antioxidant properties. In recent times, biologists, medicinal and food chemist analysis for protecting persons against these diseases discovered new and economical synthetic antioxidant compounds. Consequently, current investigations have focused on the antibacterial effects study of the newly prepared compounds. In this work, our purpose is to find out new procedures for the synthesis of significant organic compounds, [62-73] we investigated a green procedure for the preparation of some pyrrolobenzoazepine derivatives **6** via the multicomponent reactions of isatin **1**, haloketones **2**, ammonium acetate **3**, electron-deficient acetylenic compounds 4 in the presence of the catalytic amount of Ag/CdO/ZnO NCs in water at room temperature with excellent yields (Scheme **1**).

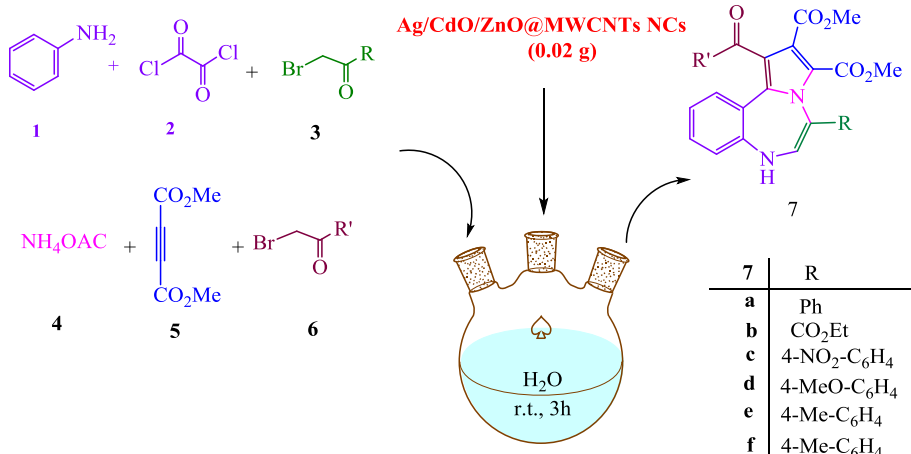

7	R	R'	Yield (%) of 7
a	Ph	4-Br-C_6H_4	87
b	CO_2Et	4-MeO-C_6H_4	93
c	4-NO_2-C_6H_4	4-MeO-C_6H_4	80
d	4-MeO-C_6H_4	4-Br-C_6H_4	90
e	4-Me-C_6H_4	4-Br-C_6H_4	90
f	4-Me-C_6H_4	4-MeO-C_6H_4	95
g	4-Me-C_6H_4	4-NO_2-C_6H_4	80
h	4-MeO-C_6H_4	CO_2Et	97
i	4-NO_2-C_6H_4	CO_2Et	90
j	CO_2Et	CO_2Et	97

Scheme 1. Synthesis of functionalized pyrrolobenzoazepines

Result and Discussion

In this research, the new pyrrolobenzoazepine derivatives **6** have been generated in high yields using five-component reactions of isatin **1**, ammonium acetate **2**, activated acetylenic compounds **3**, and haloketones **4**, **5** in the presence of Ag/CdO/ZnO NCs in water at room temperature. Ag/CdO/ZnO@MWCNTs NCs in water at room temperature. During this work, we report the ‘‘green-chemical” synthesis of Ag NPs by the reduction of Ag^{+} ions using *Petasites hybridus* rhizome aqueous extract. The adopted methodology was totally hazard free, clean, nontoxic and environment friendly. In this work, the silver metal ions were reduced to nano zero valent (NZV) metallic particles by flavonoid and phenolics present in the extract of *Petasites hybridus* rhizome according the below mechanism (Scheme 2).

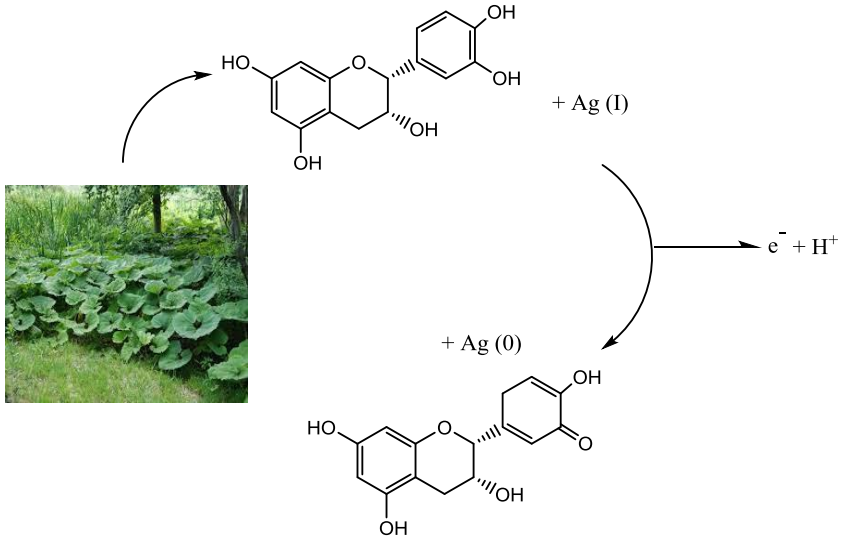

Scheme 2. Mechanism of synthesized Ag NPs using the aqueous extract of *Petasites hybridus* rhizome

The progress of the reaction between metal ions and aqueous extract of Petasites hybridus rhizome to produce the Ag NPs was monitored by recording the absorption spectra as a function of time which demonstrates the formation of Ag NPs after 10 min indicate the typical surface resonance peak of Ag NPs around 435 nm (Figure 1). Furthermore, the stability of Ag NPs was monitored by UV–vis spectroscopy at the times ranging 10 min to 15 days which shows that the synthesized Ag NPs by this procedure is completely stable even after 15 days with no considerable variance in the form, position, and symmetry of the absorption peak.

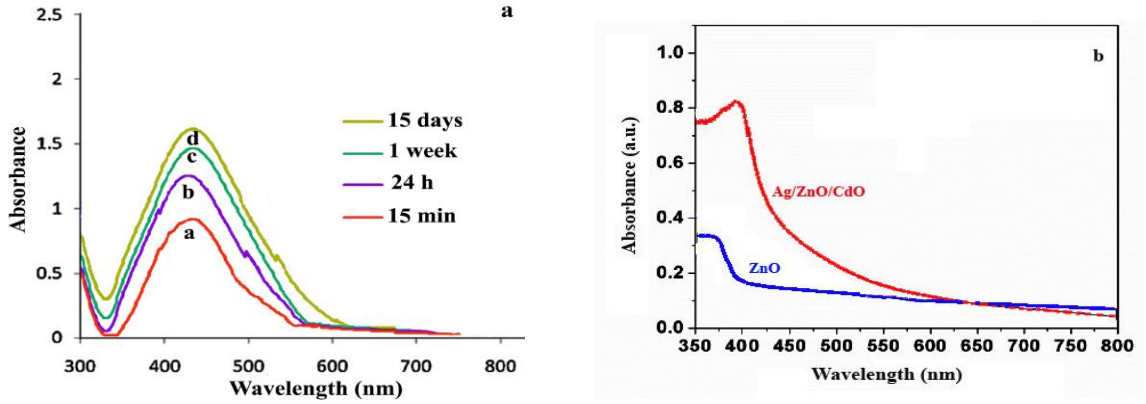

Figure 1. a) UV–vis spectrum of the Ag NPs b) UV–vis spectrum of the Ag/CdO/ZnO NCs.

Figure 1 exhibited the absorption edges of the pure ZnO nanoparticles which lies between 350-400 nm. The absorption bands of the ternary (ZnO/Ag/CdO) catalysts are broader (400- 600 nm) and it obviously shows that ZnO/Ag/CdO nanocomposite showing absorption which is red shifted compared with pure ZnO which lies in the blue region of the spectrum. It is clearly observed that the ZnO absorption edge is ~ 365 nm and the corresponding wavelength exists in the UV region. ZnO band gap value is high as compared with CdO and surface phonon resonance value of Ag. Hence, the UV-Vis absorption results indicated that the prepared ternary catalysts have absorption bands in the visible region. It is also well known that the photocatalytic process mainly depends on the wavelength of irradiated light. Therefore, the photocatalytic process by the ternary nanocomposites could be better than binary nanaocomposites under visible light irradiation.

For confirmation the structure of novel Ag/CdO/ZnO@MWCNTs NCs, we utilized SEM, XRD, EDX and TEM analysis. For determination and confirmation the construction of novel Ag/CdO/ZnO@MWCNTs NCs, we employed the scanning electron microscopy images (SEM) (Figure 2). The FE-SEM images of pure (a) Pure ZnO, b) CdO, c) Ag NPs, d) Ag/ZnO NCs, e)Ag/CdO/ZnO and f) Ag/CdO/ZnO@MWCNTs NCs samples are shown in Figure 2. FE-SEM images show the randomly distributed nanorods of uniform sizes and diameter. When compared with pure ZnO, ZnO/Ag and ternary Ag/ CdO/ZnO systems show nanorods along with spherical shape particle. It is evidently observed that the size of the nanorods decreases in the ternary nanocomposite system because of heterogeneous nucleation effect. The addition of silver and cadmium oxide may influence the size and morphology of ZnO. Compared with binary and pure system, the ternary nanocomposite nanorods are smaller in size due to the nucleation and synergetic effect.

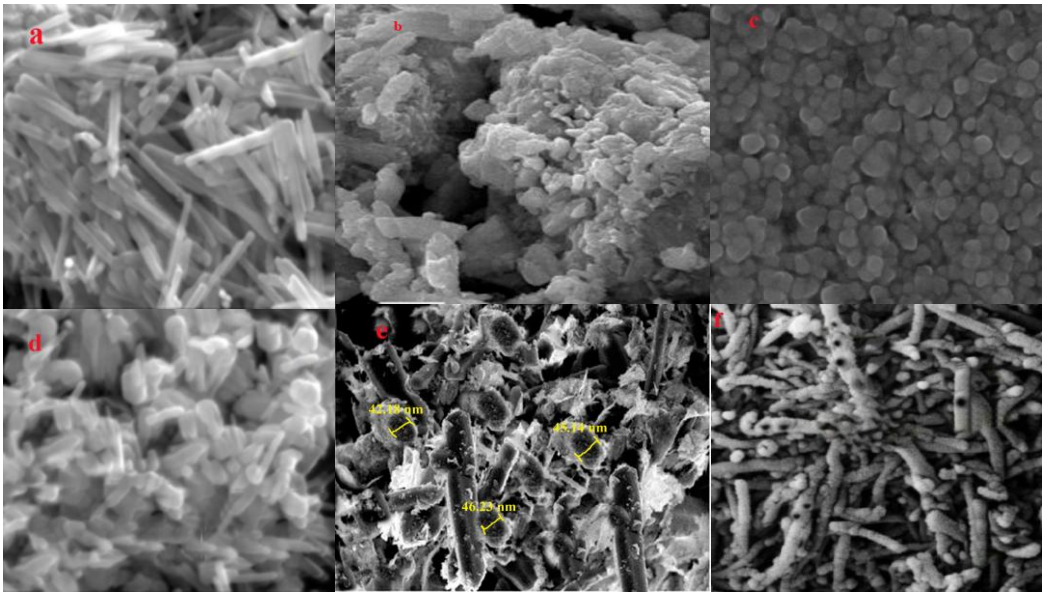

Figure 2. The SEM image of Ag/CdO/ZnO

The XRD analysis of Ag/CdO/ZnO MNCs is exhibited in Figure **3** for confirmation of the particle size (Figure **3**).

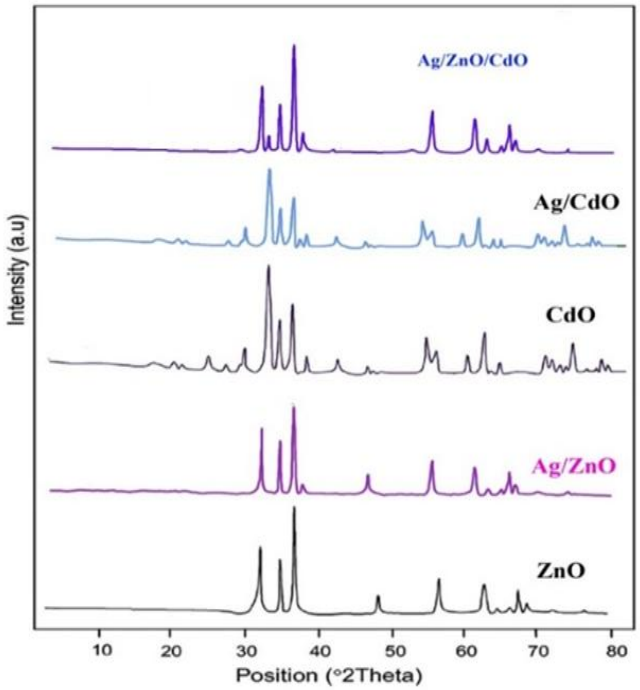

Figure 3. X-ray diffraction spectra of Ag/CdO/ZnO NCs

X-ray diffractograms (Figure **3**) show the typical XRD patterns of the ZnO, CdO, Ag/ZnO, Ag/CdO and Ag/CdO/ZnO. Characteristic peaks of ZnO at 31.7, 34.4, 36.2, and 56.6^{o} correspond to (100), (002), (101), and (110) diffraction peaks of wurtzite ZnO indicate hexagonal structure for ZnO. The lattice parameters for the pure ZnO sample matches well with the (JCPDS file no. 36-1451). The XRD pattern of Ag/ ZnO/CdO obviously shows additional peaks at 2θ=38.3, 46.2 and 64.6^{o} correspond to (111), (200) and (220) planes of face-centered cubic (fcc) lattice of metallic Ag (JCPDS file no. 04-0783) which can indicate that the Ag NPs exist in the composites and this indicates that the ZnO surface is covered with silver particles. No peaks corresponding to Ag_2O are detected. Peaks at 2θ= 33.8, 54.7 and 68.1^{o} in Ag/CdO/ZnO can be indexed to (111), (311), and (222) planes that indicate the cubic structure for cadmium oxide (JCPDS No: 73-2245). There is no remarkable shift of other diffraction peaks and no crystalline impurities are observed. The average crystallite size (D) of catalyst is estimated using Scherrer's equation:

$$D = k\lambda/\beta \cos\theta$$

Where crystallite size (nm) and crystallite shape factor (0.90) were shown by D and k respectively. X-ray wavelength for CuKα (0.15418 nm), the full-width-half-maximum (FWHM) of the peak and Bragg angle was shown by λ, β, and θ respectively. From this equation, the average crystallite size of Ag/CdO/ZnO is found to be 40 nm. All the diffraction peaks are exactly indexed and the peaks show the hexagonal structure for ZnO (JCPDS file no. 36-1451), cubic structure for Ag (JCPDS file no. 04-0783), and a cubic structure for CdO (JCPDS No.73-2245). In the binary (ZnO/Ag) and ternary (Ag/CdO/ZnO) nanocomposites was observed that the peaks were shifted towards a lower angle compared to the peaks of pure ZnO which is mark by the dotted line. The lower shift in the peaks was due to the larger ionic radius of cadmium and silver compared to that of the smaller ionic radius of zinc. However, the addition of impurity (cadmium and silver) does not affect the structure of ZnO. To further examine the morphology of the Ag/ZnO/CdO@MWCNTs NCs, the samples were considered by TEM, as displayed in Figure **4**. It can be seen that Ag/ZnO/CdO NCs are supported on the MWCNTs.

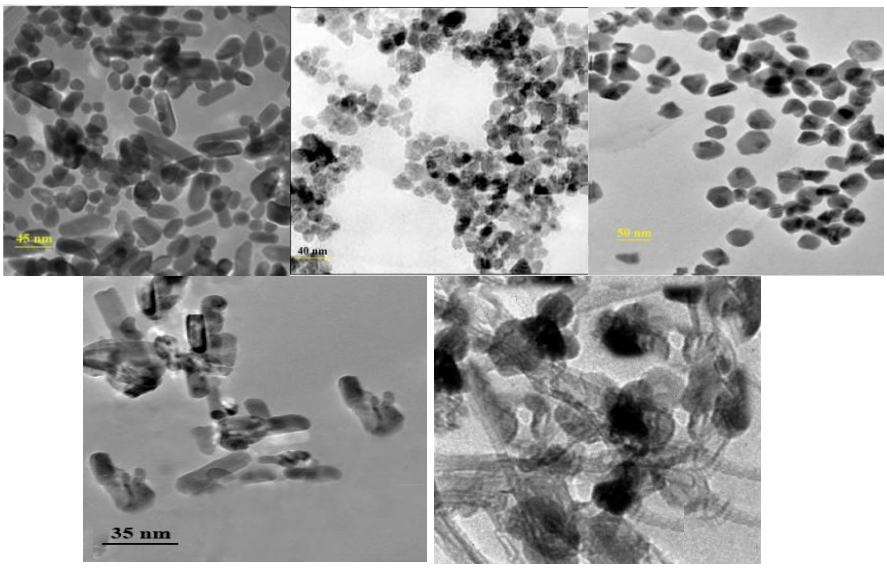

Figure 4. TEM image of synthesized catalyst

The TEM image (Figure 4) of ZnO/Ag/CdO nanocomposite is in agreement with the results of FE-SEM, which also showed nanorods along with closely attached spherical shaped nanoparticles.

The elemental composition of green Ag/CdO/ZnO NCs was investigated by the Energy dispersive X-ray spectroscopy (EDS) spectrum. It was confirmed that Ag/CdO/ZnO NCs were consisted of Cd, Ag, Zn and oxygen (Figure **5**).

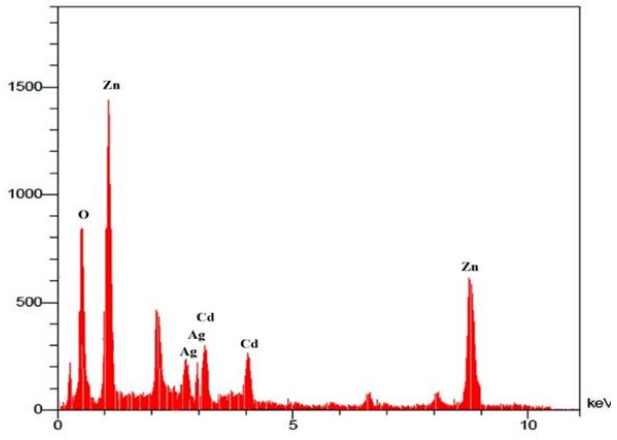

Figure 5. The EDS image of green Ag/CdO/ZnO NCs

We also evaluated the catalytic activities of the Ag/CdO/ZnO NCs through the synthesis of pyrrolobenzoazepine derivatives in the presence Ag/CdO/ZnO NCs. The important section in this research is the optimization of reaction condition. For this reason, initially, the reaction of isatin **1**, ammonium acetate **2**, dimethyl acetylenedicarboxylate **3**, phenacyl bromide **4a** and 4-bromphenacyl bromide **5a** was utilized as a sample reaction (Table 2). This reaction wasn't carried out without catalyst even after 12 h and in this condition the mixture of reaction has many byproducts and caused to busy of reaction medium (entry 1, 2, Table 2). Sabbaghan and Hossaini have performed similar reactions without the catalyst that led to generating of *N*-alkyl 2-[(2-oxo-2-aryl ethyl) amino] benzamide derivatives.[80] For this reason, Et_3N (0.02 g) was added as a sample catalyst to the mixture of reactions. The yield of 6**a** was achieved 58% after 5 h (entry 3 Table 2). other catalysts such as pyridine, K_2CO_3, Ag/CdO NPs, ZnO NRs, Pyridine, Ag/ZnONPs and Ag/CdO/ZnO NCs, are evaluated in the sample reaction for more investigation the effect of catalyst. As a result, these outcomes exhibited the Ag/CdO/ZnO NCs are the best catalyst for this reaction.

Table 1. Investigation of solvent, catalyst and temperature effect on the condensation reaction of compound **6a**

Entry	Catalyst	Catalyst amount (g)	Solvent[a]	Temp.[b]	Time (h)[c]	Yield (%)[d]
1	-	-	-	r.t.	12	trace
2	-	-	EtOH	100	12	trace
3	Et_3N	0.015	EtOH	r.t.	5	30
4	Et_3N	0.02	EtOH	r.t.	4	35
5	Et_3N	0.02	EtOH	100	4	35
6	Et_3N	0.02	H_2O	r.t.	3	37
7	Et_3N	0.02	CH_3CN	r.t.	3	45
8	Pyridine	0.02	H_2O	r.t.	3	20
9	Pyridine	0.02	CH_3CN	r.t.	3	45
10	K_2CO_3	0.02	H_2O	r.t.	6	35
11	K_2CO_3	0.02	CH_3CN	r.t.	5	20
12	K_2CO_3	0.02	EtOH	r.t.	5	25
13	Ag/CdO NPs	0.02	H_2O	r.t.	4	65
14	Ag/ZnO NPs	0.02	CH_3CN	r.t.	4	65
15	Ag/ZnO NPs	0.02	EtOH	r.t.	4	60
16	**Ag/CdO/ZnO NCs**	**0.02**	**H_2O**	**r.t.**	**4**	**75**
17	**Ag/CdO/ZnO NCs**	0.015	**H_2O**	**r.t.**	**3**	**70**
18	**Ag/CdO/ZnO NCs**	0.02	**H_2O**	**r.t.**	**3**	**75**
19	**Ag/CdO/ZnO NCs**	0.02	**H_2O**	**100**	**3**	**80**
20	**Ag/CdO/ZnO NCs**	0.02	CH_3CN	r.t.	3	68
21	**Ag/CdO/ZnO NCs**	0.02	Toluene	100	3	70
22	**Ag/CdO/ZnO NCs**	**0.025**	**H_2O**	**r.t.**	**3**	**75**
23	ZnO (NRs)	0.02	H_2O	r.t.	3	45
24	ZnO (NRs)	0.02	CH_3CN	r.t.	3	50

[a]The amount of solvent was 5 mL.
[b]Temperature (^oC) for reaction conditions
[c]Time (h) for reaction conditions
[d]Isolated yield

When Ag/CdO NPs and Ag/ZnO NPs were used as a separate catalysts, the yields were lower than Ag/CdO/ZnO NCs (Table 1, entries 13 and 14). As shown in outcomes, different amounts of catalyst Ag/CdO/ZnO (0.015-0.025g) were utilized the discovering the best amounts of catalyst. The results of the investigation displayed that 0.02 g is the best amount of catalyst for this reaction. By increasing the amount of catalyst from 0.02 g, didn't see any significant variation in the yields of reaction (entry 17, 20, Table 1). Also, by raising the reaction temperature to 100 ^oC the yield of 6a was not altered (entry 4, 5, Table 1). the yield of product 6a was obtained in 75 % yield after 3 h (entry 17, Table 2) in the best conditions. As shown in Table 1, the Ag/CdO/ZnO NCs (0.02 g) as a catalyst, H2O as and room temperature are the best conditions for preparation of 6a. The outcomes in Table 2 displayed the Ag/CdO/ZnO NCs were employed five times in sample reaction (the preparation of pyrrolobenzoazepine 6a) without any significant variations in the yield of 6a. The catalyst was separated after each run, washed with water, dried at environment temperature, and used again in model reaction for confirmation of the reusability of catalyst.

Table 2: Reusability of Ag/CdO/ZnO NCs in the synthesis of compound **6a**

Run	1	2	3	4	5	6
Compound 6a yield (%)	75	75	73	72	72	66

IR, ^{1}H NMR, ^{13}C NMR, and mass spectral data are used for investigation and confirmation of the structures of pyrrolobenzoazepine **6**. For instance, the 1H NMR spectrum of 6a displayed two singlets at δ= 3.78 and 3.92 ppm for methoxy protons, one singlet at 7.36 for methine proton, two singlet at 10.24 and 12.34 ppm for NH proton along with signals for aromatic protones at 7.06-7.95 ppm. The carbonyl group resonance of 6a was detected at 161.2, 163.8 and 189.3ppm in the 13C NMR spectrum. The characteristic C=O bands were shown in IR spectrum of **6a** and the mass spectrum of 6a has displayed the molecular ion peak at m/z = 557. Although there aren't any records for the details of the reaction mechanism, the suggested mechanism for these reactions is investigated in Scheme **2**. It is supposable that the reaction begins with the formation of imine **7** by reacting between isatin 1 and ammonium acetate **2** in the presence of Ag/CdO/ZnO NCs as the catalyst. The intermediate **7** react with dimethyl acetylene dicarboxylate **3** to generate the intermediate **8** which react with alkyl bromides **4** and produce intermediate **10** with elimination of HBr in the presence of catalyst. Intermolecular cyclization reactions of intermediate **10** along with the elimination of carbon monoxide produce compounds **13**. Intermediate **13** in the presence of catalyst react with alkyl bromides **5** and produce intermediate **14** which by elimination of HBr and cyclization of intermediate 15 along with elimination of water produce compounds **6**.

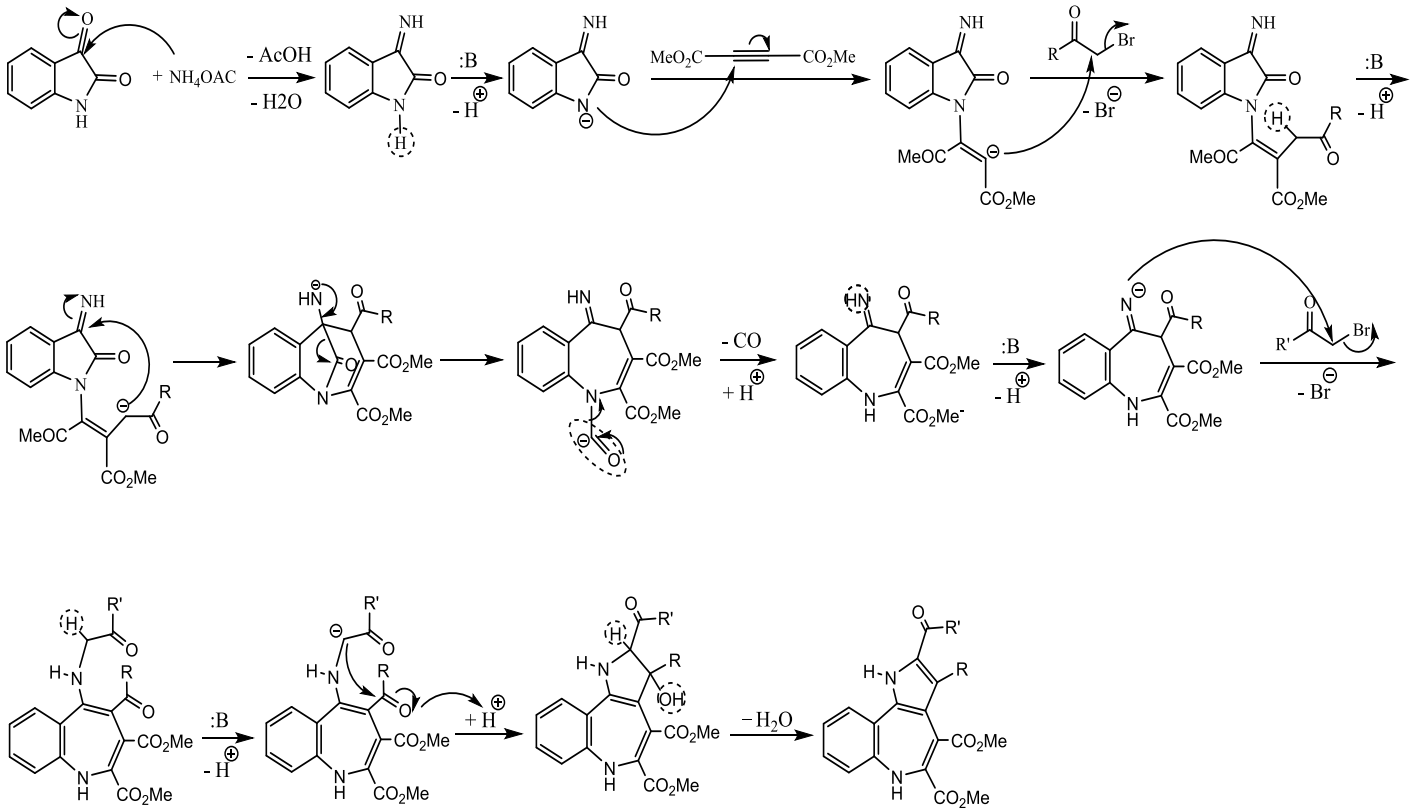

Scheme 2. Plausible mechanism for the production of **6**

Diphenyl-2-picrylhydrazyl (DPPH) utilizing for evaluation of antioxidant ability of pyrrolobezadiazepines

DPPH radical trapping examin is broadly utilized for the approval the power of synthezied compounds to get free radicals and its antioxidant property in foods and biological structures. In these valuation, antioxidant ability of prepared pyrrolobezadiazepines was proved by taking the hydrogen atom or one electron by DPPH radical. The synthesized compounds have NH groups and because of having acidic hydrogen have antioxidant activity. The antioxidant activity of investigated compounds **6a-6d** has not much different from each other. In general antioxidant activity of these compounds are due to having NH groups. The percentage of DPPH free radical trapping indicates the antioxidant degree of the synthesized pyrrolobezadiazepines **6a-6d**. In other words, the order of antioxidant ability of pyrrolobezadiazepines **6a-6d** is determined basis of the electron or hydrogen donating power of pyrrolobezadiazepines to the DPPH radical. When DPPH give one electron or hydrogen from antioxidant or a radical typs, its absorbtion was decreased from 517 nm. In this research, the ability of getting free radicals by pyrrolobezadiazepines **6a-6d** was compared with BHT and TBHQ as standard syntheiszed antioxidant at different concentrations. In general, the order of antioxidant activity of some synthesized pyrrolobezadiazepines **6a-6d** is TBHQ> BHT>**6a**>**6c>6b>6d** (Figure 6).

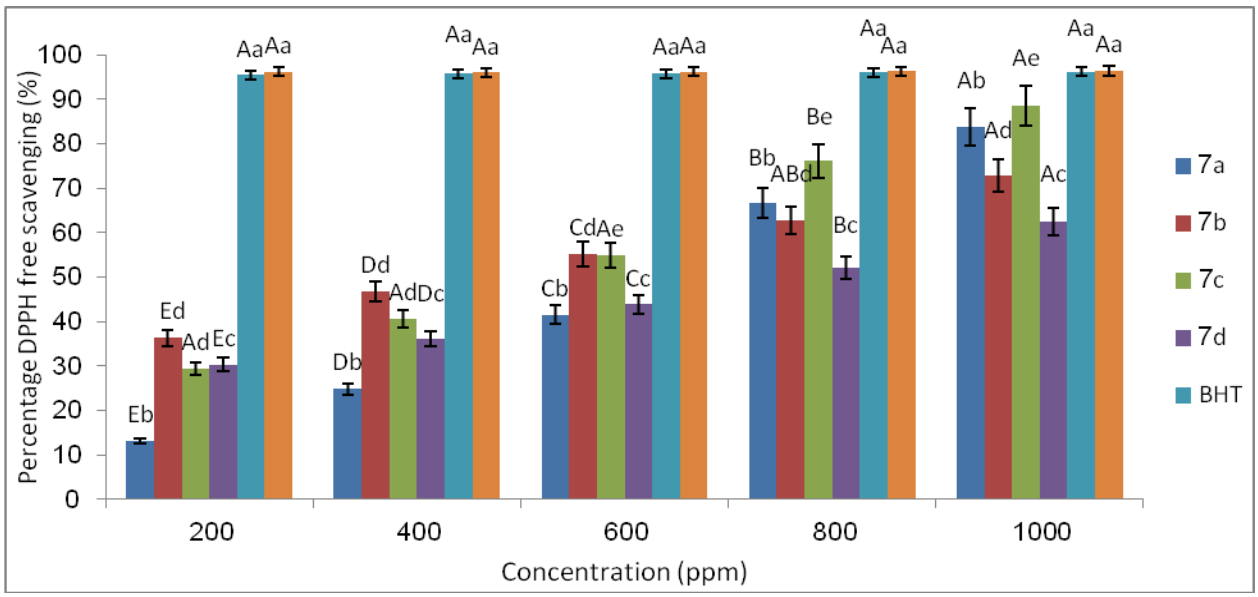

Figure 6. Radical scavenging activity (RSA) of **6a-6d**.

Good difference relative to BHT and TBHQ existed in all concentrations of the new prepared pyrrolobezadiazepines derivatives that are showed in Figure 8. In among investigated s pyrrolobezadiazepines **7a** exhibited good activity for trapping of radical relative to BHT and TBHQ as standard antioxidant.

Ferric ions (Fe^{3+}) reducing potential (FRAP)

The calculating reducing quantity of Fe^{3+}/ferricyanide to the Fe^{2+}/ ferrous at 700 nm is important factor for ferric ions (Fe^{3+}) reducing ability of some synthesized pyrrolobezadiazepines such as **6a-6d**. Among the investigated pyrrolobezadiazepines **6a** was displayed good reducing ability than to BHT and TBHQ as standard antioxidants (Figure 9). The order of reducing activity of the investigated pyrrolobezadiazepines is: TBHQ> BHT>**6a**>**6c>6b>7d**. The outcomes are displayed in Figure 7.

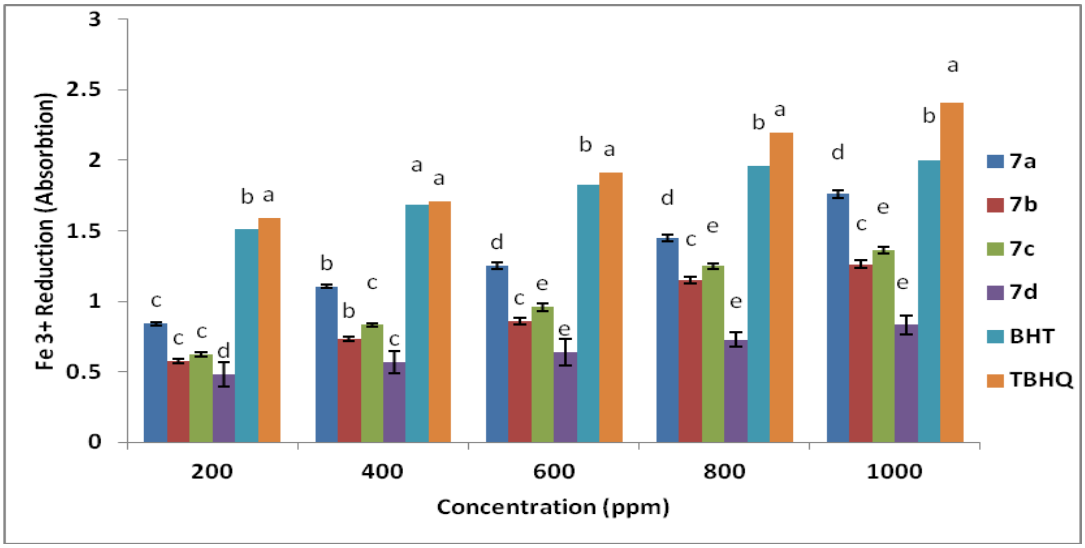

Figure 7. Ferric ions (Fe^{3+}) reducing antioxidant power (FRAP) of compounds **6a-6d**

The thermal properties of synthesized composites were investigated by thermo gravimetric analysis (TGA) as shown in Figure 8. Eventual MWCNTs oxidation is expected to form CO_2 gas, leaving the sample and resulting in composite weight loss as a function of temperature. It was investigated in the 25–800 ^{o}C temperature range. There is no weight loss in the range 0–350 ^{o}C, which indicates the absence of coordinated or uncoordinated water molecules. The weight loss above 450 °C is due to MWCNTs decomposition.

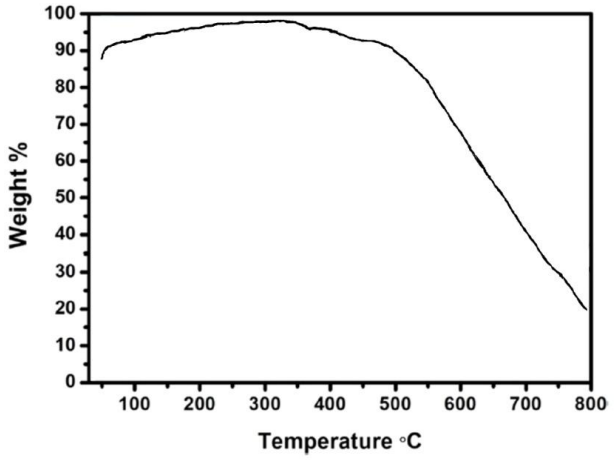

Figure 8. The TGA curve of green Ag/CdO/ZnO@MWCNTs

The pore structure of the Ag/ZnO/CdO@MWCNTs nanocomposite sample was investigated by nitrogen adsorption–desorption isotherms and the pore size distribution was calculated by BJH method according to the desorption branch. It is well known that when size of the catalyst will decrease, the surface area will be increased, the same trend has been observed in this work, which is confirmed by BET analysis as shown in Table 3. The ternary Ag/ ZnO/CdO@MWCNTs nanocomposite shows highest surface area (Table 1) compared with binary nanocomposites (ZnO/Ag and ZnO/CdO) and pure ZnO. The difference in their surface area was due to the synergetic effect among the components such as ZnO, Ag, CdO and MWCNTs in the composite system. The increase in the surface area was significant, hence, the larger surface area of Ag/ZnO/CdO@MWCNTs nanocomposite will benefit the spatial separation of redox sites in the crystals which can enhance electron-transfer properties of the nanocomposite.

Table 3. Nitrogen adsorption–desorption data of the catalysts.

Catalysts	Surface area BET (m^2/g)	Pore Volume (cm^3/g)	Pore diameter (nm)
MWCNTs	201.7234	0.5239	12.3412
ZnO	10.7145	0.0268	32.6703
ZnO/CdO	13.8023	0.08313	26.8312
Ag/ZnO/CdO	21.6347	0.1924	18.3245
Ag/ZnO/CdO@MWCNTs	87.4852	0.3557	11.9714

Conclusions

The Ag/CdO/ZnO NCs as a new heterogeneous nanocatalyst was prepared and characterized using XRD, FESEM, EDX and TEM analyses. The nanocatalyst performance was tested by performing the one-pot synthesis of a new family of substituted pyrrolobenzoazepines via the condensation reactions of isatin, ammonium acetate, α-haloketones and activated acetylenic compounds in water at room temperature. The advantages of this procedure are: the one-pot operation, excellent yields of product in short reaction time, abundant and eco-friendly of catalyst. High atom economy and yield, mild and clean reaction condition, low catalyst loading, and short reaction time are some advantages of this procedure for synthesis of pyrroloazepines.

Experimental

General

All materials employed in this work were purchased from Fluka and Merck with no further purification. The structure of Ag/CdO/ZnO NCs was confirmed by XRD, SEM, EDX and. X-ray diffraction patterns (XRD) was performed for calculating of the size of prepared Ag/CdO/ZnO NCs. The Scherrer's formula; $D= 0.9\lambda/\beta \cos\theta$ used for calculating the average crystallite size of Ag/CdO/ZnO NCs, where D is the diameter of the nanoparticles, λ (CuK_α) =1.5406 Å and β is the full-width at half-maximum of the diffraction lines. FT-IR spectra were recorded by a Shimadzu IR-460 spectrometer for synthesized compounds. Also, the ^1H and ^{13}C NMR spectra are used for the structure confirmation of synthesized compounds by BRUKER DRX-500 AVANCE spectrometer at 500.1 and 125.8 MHz respectively using TMS as the internal standard or 85% H_3PO_4 as the external standard for solution in $CDCl_3$. A FINNIGAN-MAT 8430 spectrometer with an ionization potential of 70 eV utilized for Mass spectra.The elemental analysis C, H, and N for synthesized compounds was carried out by a Heraeus CHN–O-Rapid analyzer. Energy-dispersive X-ray Spectroscopy (EDX) was performed by Mira 3-XMU FESEM (Tescan Co, Brno, Czech Republic). The instrument was used for TEM analysis are: Instrument model: CM120; Manufacturing Country: Netherlands.

Preparation of CdO/ZnO nanoparticles

Cd $(NO_3)_2$ (1.5 g) and $ZnCl_2.4H_2O$ (1.5 g) was solved in *Petasites hybridus* rhizome water extract (30 mL) at 100 ^oC in round bottom flask for 5 h. Then it was cooled to room temperature, sonicated for 30 min and was centrifuged at 7000 rpm for about 10 min for removing the unwanted organic matters and then was filtered. The precipitate was filtered and washed with distilled water and ethanol (96%) for several times. The samples were then heated at 300 °C for 1 h. Produced bio-CdO/ZnO nanoparticles (bio-CdO/ZnO NPs) were dried in the air at room temperature for 24 h.

Green synthesis of Ag/CdO/ZnO NCs

In a typical method, 0.1 g of prepared CdO/ZnO NPs and $AgNO_3$ (1.5 g) and was dispersed in 100 mL *Petasites hybridus* rhizome water extract and the mixture was sonicated at 100 ºC for 45 min. After cooling at r.t., the product was separated by filtration and washed several times with water and ethanol respectively to afford the Ag/CdO/ZnO NCs.

General procedure for the preparation of (6a-6i)

The mixture of the isatin **1 (**1 mmol, 0.147 g) and the ammonium acetate **2** (1 mmol) was stirred in the presence of Ag/CdO/ZnO NCs (0.02 g) as catalyst in water at room temperature for 30 min. After this time, activated acetylenic compounds **3** (1 mmol) was added

to the mixture and stirred for 45 min. Then alkyl bromides **4** (1 mmol) was added and allow new mixture was stirred for 45 min. After this time α-haloketones **5** (1 mmol) was added to mixture of reaction and allow to new mixture was mixed for one hour. After completion of reaction that was monitored by (TLC control (hexane–AcOEt, 4:1), the solid was separated by filtration and washed with EtOAC (Ethylacetate) for separating of catalyst. Then the column chromatography [silica gel (230–240 mesh; Merck), hexane/EtOAc 6:1] employed for purification of the residue to afforded pure title compounds.

Dimethyl 2-(4-bromobenzoyl)-3-phenyl-1,6-dihydrobenzo[b]pyrrolo[2,3-d]azepine-4,5-dicarboxylate (6a):

Yellow powder, mp 143-145˚C, 0.97 g,Yield 75%; FT-IR (KBr) (γ_{max}/cm^{-1}): 3193, 1703, 1672, 1693, 1607, 1531, 1261 cm^{-1}. ^{1}H NMR (500 MHz, $CDCl_3$): δ= 3.78 (3 H, s, MeO), 3.92 (3 H, s, MeO), 7.06 (1 H, d, ^3J =7.6 Hz, CH), 7.12 (2 H, d, ^3J = 7.6 Hz, 2 CH),7.23 (1 H, t, ^3J = 7.6 Hz, CH), 7.32 (2 H, t, ^3J = 7.6 Hz, 2 CH), 7.43 (1 H, t, ^3J = 7.6 Hz, CH), 7.52 (1 H, d, ^3J = 7.6 Hz, CH), 7.63 (1 H, t, ^3J = 7.6 Hz, CH), 7.73 (2 H, d, ^3J = 7.8 Hz, 2 CH), 7.95 (2 H, d, ^3J = 7.8 Hz, 2 CH), 10.24 (1 H, s, NH), 12.34 (1 H, s, NH) ppm. ^{13}C NMR (125.6 MHz, $CDCl_3$): δ = 51.3 (MeO), 52.4 (MeO), 103.4 (C), 108.3 (C), 112.3 (CH), 113.2 (C), 114.5 (C), 119.2 (CH), 123.2 (CH), 124.8 (CH), 125.3 (CH), 127.2 (2 CH), 128.3 (2 CH), 129.4 (2 CH), 131.2 (C), 132.0 (2 CH), 132.7 (CH), 134.4 (C), 137.2 (C), 138.5 (C), 140.2 (C), 144.3 (C), 161.2 (C=O), 163.8 (C=O), 189.3 (C=O) ppm. EI-MS: 557 (M$^+$, 10), 526 (46), 31 (100). Anal. Calcd. for $C_{29}H_{21}BrN_2O_5$ (557.39): C, 62.49; H, 3.80; N, 5.03; found: C, 62.63; H, 3.92; N, 5.18%.

3-Ethyl 4,5-dimethyl 2-(4-methoxybenzoyl)-1,6-dihydrobenzo[b]pyrrolo[2,3-d]azepine-3,4,5-tricarboxylate (6b):

Yellow powder, mp 123-125˚C, 0.93 g, Yield 73%; FT-IR (KBr) (γ_{max}/cm^{-1}): 3174, 1708, 1673, 1434, 138, 1272 cm^{-1}. ^{1}H NMR (500 MHz, $CDCl_3$): δ= 1.25 (3 H, t, ^3J = 7.4 Hz, CH_3), 3.75 (3 H, s, MeO), 3.87 (3 H, s, MeO), 3.93 (3 H, s, MeO), 4.16 (2 H, q, ^3J = 7.4 Hz, CH_2O), 7.05 (2 H, d, ^3J =7.7 Hz, 2 CH), 7.15 (1 H, d, ^3J = 7.6 Hz, CH),7.21 (1 H, t, ^3J = 7.7 Hz, CH), 7.34 (1 H, d, ^3J = 7.6 Hz, CH), 7.45 (1 H, t, ^3J = 7.6 Hz, CH), 7.78 (2 H, d, ^3J = 7.8 Hz, 2 CH), 10.32 (1 H, s, NH), 12.25 (1 H, s, NH) ppm. ^{13}C NMR (125.6 MHz, $CDCl_3$): δ = 13.8 (CH_3), 51.7 (MeO), 52.5 (MeO), 55.7 (MeO), 61.4 (CH_2O), 101.7 (C), 112.8 (2 CH), 114.2 (C), 117.3 (C), 118.5 (C), 119.2 (CH), 120.4 (CH), 123.4 (CH), 124.5 (CH), 131.2 (CH), 132.5 (2 CH), 133.4 (C), 135.7 (C), 136.5 (C), 143.6 (C), 158.2 (C), 160.7 (C=O), 164.2 (C=O), 165.8 (C=O), 188.7 (C=O) ppm. EI-MS: 504 (M$^+$, 15), 473 (46), 31 (100). Anal. Calcd. for $C_{27}H_{24}N_2O_8$ (504.49): C, 64.28; H, 4.80; N, 5.55; found: C, 64.43; H, 4.92; N, 5.67%.

Dimethyl 2-(4-methoxybenzoyl)-3-(4-nitrophenyl)-1,6-dihydrobenzo[b]pyrrolo[2,3-d]azepine-4,5-dicarboxylate (6c):

Yellow powder, mp 168-170˚C, 0.88 g,Yield 71%; FT-IR (KBr) (γ_{max}/cm^{-1}): 3278, 1708, 1673, 1434, 1381, 1272 cm^{-1}. ^{1}H NMR (500 MHz, $CDCl_3$): δ= 3.73 (3 H, s, MeO), 3.86 (3 H, s, MeO), 3.95 (3 H, s, MeO), 7.02 (2 H, d, ^3J =7.8 Hz, 2 CH), 7.14 (1 H, d, ^3J = 7.7 Hz, CH),7.24 (1 H, t, ^3J = 7.7 Hz, CH), 7.37 (1 H, d, ^3J = 7.7 Hz, CH), 7.42 (1 H, t, ^3J = 7.7 Hz, CH), 7.68 (2 H, d, ^3J = 7.8 Hz, 2 CH), 7.75 (2 H, d, ^3J = 7.8 Hz, 2 CH), 7.85 (2 H, d, ^3J = 7.8 Hz, 2 CH), 10.16 (1 H, s, NH), 12.38 (1 H, s, NH) ppm. ^{13}C NMR (125.6 MHz, $CDCl_3$): δ = 51.4 (MeO), 52.6 (MeO), 55.6 (MeO), 109.2 (C), 111.4 (CH), 112.4 (2 CH), 113.5 (C), 114.6 (C), 115.3 (C), 119.2 (CH), 123.4 (CH), 125.5 (CH), 127.5 (2 CH), 130.2 (2 CH), 131.3 (CH), 132.4 (2 CH), 134.2 (C), 135.3 (C), 137.6 (C), 142.2 (C), 143.8 (C), 146.3 (C), 159.2 (C), 160.6 (C=O), 164.3 (C=O), 189.5 (C=O) ppm. EI-MS: 553 (M$^+$, 10), 522 (58), 31 (100). Anal. Calcd. for $C_{30}H_{23}N_3O_8$ (553.52): C, 65.10; H, 4.19; N, 7.59; found: C, 65.23; H, 4.28; N, 7.68%.

Dimethyl 2-(4-bromobenzoyl)-3-(4-methoxyphenyl)-1,6-dihydrobenzo[b]pyrrolo[2,3-d]azepine-4,5-dicarboxylate (6d):

Yellow powder, mp 161-163˚C, 1.06 g, Yield 75%; FT-IR (KBr) (γ_{max}/cm^{-1}): 3195, 1718, 1676, 1493, 1374, 1272 cm^{-1}. ^{1}H NMR (500 MHz, $CDCl_3$): δ= 3.78 (3 H, s, MeO), 3.83 (3 H, s, MeO), 3.95 (3 H, s, MeO), 6.95 (2 H, d, ^3J =7.8 Hz, 2 CH), 7.06 (1 H, d, ^3J = 7.6 Hz, CH), 7.12 (1 H, t, ^3J = 7.6 Hz, CH), 7.23 (1 H, d, ^3J = 7.6 Hz, CH), 7.38 (2 H, d, ^3J = 7.8 Hz, 2 CH), 7.45 (1 H, t, ^3J = 7.6 Hz, CH), 7.73 (2 H, d, ^3J = 7.8 Hz, 2 CH), 7.98 (2 H, d, ^3J = 7.8 Hz, 2 CH), 10.34 (1 H, s, NH), 12.32 (1 H, s, NH) ppm. ^{13}C NMR (125.6 MHz, $CDCl_3$): δ = 51.2 (Me), 52.5 (MeO), 55.6 (MeO), 104.3 (C), 109.5 (C), 111.5 (CH), 112.3 (2 CH), 114.2 (C), 115.3 (C), 119.2 (CH), 123.8 (CH), 126.2 (CH), 127.7 (2 CH), 128.5 (2 CH), 130.2 (C), 131.4 (C), 132.4 (2 CH), 133.2 (CH), 134.5 (C), 137.2 (C), 140.3 (C), 144.3 (C), 155.8 (C), 161.2 (C=O), 166.7 (C=O), 190.6 (C=O) ppm. EI-MS: 587 (M$^+$, 10), 556 (68), 31 (100).

Anal. Calcd. for $C_{30}H_{23}BrN_2O_6$ (587.42): C, 61.34; H, 3.95; N, 4.77; found: C, 61.48; H, 4.08; N, 4.86%.

Dimethyl 2-(4-bromobenzoyl)-3-(p-tolyl)-1,6-dihydrobenzo[b]pyrrolo[2,3-d]azepine-4,5-dicarboxylate (6e):

Yellow powder, mp 156-158˚C, 1.03 g, Yield 72%; FT-IR (KBr) (γ_{max}/cm^{-1}): 3371, 1718, 1673, 1506, 1374, 1210 cm^{-1}. ^{1}H NMR (500 MHz, $CDCl_3$): δ= 2.36 (3 H, s, Me), 3.75 (3 H, s, MeO), 3.94 (3 H, s, MeO), 7.04 (1 H, d, ^3J =7.6 Hz, CH), 7.12 (1 H, t, ^3J = 7.6 Hz, CH), 7.22 (2 H, d, ^3J = 7.8 Hz, 2 CH), 7.35 (1 H, d, ^3J = 7.6 Hz, CH), 7.43 (1 H, t, ^3J = 7.6 Hz, CH), 7.72 (2 H, d, ^3J = 7.8 Hz, 2 CH), 7.96 (2 H, d, ^3J = 7.8 Hz, 2 CH), 10.43 (1 H, s, NH), 12.42 (1 H, s, NH) ppm. ^{13}C NMR (125.6 MHz, $CDCl_3$): δ = 21.3 (Me), 51.6 (MeO), 52.7 (MeO), 104.2 (C), 109.3 (C), 111.6 (CH), 114.6 (C), 115.7 (C), 119.2 (CH), 123.6 (CH), 125.8 (CH), 127.6 (2 CH), 128.3 (2 CH), 129.6 (2 CH), 130.8 (C), 131.8 (CH), 132.7 (2 CH), 134.6 (C), 135.8 (C), 136.4 (C), 137.8 (C), 140.2 (C), 144.3 (C), 160.8 (C=O), 165.2 (C=O), 190.4 (C=O) ppm. EI-MS: 553 (M$^+$, 15), 540 (76), 31 (100). Anal. Calcd. for $C_{30}H_{23}BrN_2O_5$ (571.42): C, 63.06; H, 4.06; N, 4.90; found: C, 63.17; H, 4.18; N, 5.03%.

Dimethyl 3-(4-methoxyphenyl)-2-(4-methylbenzoyl)-1,6-dihydrobenzo[b]pyrrolo[2,3-d]azepine-4,5-dicarboxylate (6f):

Pale yellow powder, mp 147-149˚C, 0.99 g, Yield 73%; FT-IR (KBr) (γ_{max}/cm^{-1}): 3295, 1715, 1674, 1469, 1377, 1209 cm^{-1}. ^{1}H NMR (500 MHz, $CDCl_3$): δ= 2.32 (3 H, s, Me), 3.73 (3 H, s, MeO), 3.87 (3 H, s, MeO), 3.96 (3 H, s, MeO), 6.98 (2 H, d, ^3J =7.7 Hz, 2 CH), 7.05 (1 H, d, ^3J = 7.6 Hz, CH), 7.13 (1 H, t, ^3J = 7.6 Hz, CH), 7.24 (2 H, d, ^3J = 7.7 Hz, 2 CH), 7.32 (1 H, d, ^3J = 7.6 Hz, CH), 7.43 (2 H, d, ^3J = 7.7 Hz, 2 CH), 7.56 (1 H, t, ^3J = 7.6 Hz, CH), 7.78 (2 H, d, ^3J = 7.7 Hz, 2 CH), 10.08 (1 H, s, NH), 12.23 (1 H, s, NH) ppm. ^{13}C NMR (125.6 MHz, $CDCl_3$): δ = 21.7 (Me), 51.2 (MeO), 52.4 (MeO), 55.2 (MeO), 109.3 (C), 111.3 (CH), 112.4 (2 CH), 113.6 (C), 114.5 (C), 115.2 (C), 119.6 (CH), 123.3 (CH), 125.4 (CH), 129.7 (2 CH), 130.8 (CH), 131.4 (2 CH), 132.5 (2 CH), 133.6 (C), 134.8 (C), 135.2 (C), 136.3 (C), 137.3 (C), 144.5 (C), 158.6 (C), 160.5 (C=O), 164.8 (C=O), 189.4 (C=O) ppm. EI-MS: 522 (M$^+$, 15), 491 (86), 31 (100). Anal. Calcd. for $C_{31}H_{26}N_2O_6$ (522.55): C, 71.25; H, 5.02; N, 5.36; found: C, 71.38; H, 5.16; N, 5.47%.

dimethyl 1-(4-nitrobenzoyl)-5-(p-tolyl)-7H-benzo[f]pyrrolo[1,2-d][1,4]diazepine-2,3-dicarboxylate (6g):

Yellow powder, mp 175-177˚C, 0.86 g,Yield 80%; FT-IR (KBr) (γ_{max}/cm^{-1}): 3365, 1740, 1727, 1695, 1587, 1486, 1294 cm^{-1}. ^{1}H NMR (500 MHz, $CDCl_3$): δ= 2.37 (3 H, s, Me), 3.78 (3 H, s, MeO), 3.87 (3 H, s, MeO), 7.12 (1 H, d, ^3J =7.6 Hz, CH), 7.18 (1 H, t, ^3J = 7.6 Hz, CH), 7.25 (2 H, d, ^3J = 7.8 Hz, 2 CH), 7.36 (1 H, s, CH), 7.47 (1 H, d, ^3J = 7.6 Hz, CH), 7.56 (1 H, t, ^3J = 7.6 Hz, CH), 7.67 (2 H, d, ^3J = 7.8 Hz, 2 CH), 7.73 (2 H, d, ^3J = 7.8 Hz, 2 CH), 8.12 (2 H, d, ^3J = 7.8 Hz, 2 CH), 12.47 (1 H, s, NH) ppm. ^{13}C NMR (125.6 MHz, $CDCl_3$): δ = 21.5 (Me), 51.6 (MeO), 52.3 (MeO), 110.2 (C), 112.3 (CH), 113.6 (C), 114.8 (C), 118.3 (C), 120.2 (CH), 122.5 (2 CH), 123.5 (CH), 126.3 (CH), 127.8 (2 CH), 130.3 (2 CH), 131.7 (CH), 132.6 (2 CH), 133.4 (C), 135.2 (C), 136.8 (C), 138.3 (C), 145.7 (C), 147.2 (C), 152.6 (C), 162.4 (C=O), 165.4 (C=O), 189.7 (C=O) ppm. EI-MS: 537 (M$^+$, 15), 506 (68), 31 (100). Anal. Calcd. for $C_{30}H_{23}N_3O_7$ (537.52): C, 67.03; H, 4.31; N, 7.82; found: C, 67.23; H, 4.52; N, 8.03%.

Dimethyl1-(2-ethoxy-2-oxoacetyl)-5-(4-methoxyphenyl)-7H-benzo[f]pyrrolo[1,2-d][1,4] diazepine-2,3-dicarboxylate (7h):

Yellow powder, mp 136-138˚C, 0.98 g, Yield 97%; FT-IR (KBr) (γ_{max}/cm^{-1}): 3564, 1742, 1727, 1697, 1595, 1496, 1295 cm^{-1}. ^{1}H NMR (500 MHz, $CDCl_3$): δ= 1.32 (3 H, t, ^3J = 7.4 Hz, CH_3), 3.78 (3 H, s, MeO), 3.87 (3 H, s, MeO), 3.95 (3 H, s, MeO), 4.25 (2 H, q, ^3J = 7.4 Hz, CH_2O), 7.08 (2 H, d, ^3J =7.8 Hz, 2 CH), 7.15 (1 H, d, ^3J = 7.6 Hz, CH), 7.27 (1 H, t, ^3J = 7.6 Hz, CH), 7.32 (1 H, s, CH), 7.43 (2 H, d, ^3J = 7.8 Hz, 2 CH), 7.47 (1 H, d, ^3J = 7.6 Hz, CH), 7.56 (1 H, t, ^3J = 7.6 Hz, CH), 12.32 (1 H, s, NH) ppm. ^{13}C NMR (125.6 MHz, $CDCl_3$): δ = 14.3 (CH_3), 51.5 (MeO), 52.5 (MeO), 55.6 (MeO), 62.4 (CH_2O), 110.5 (CH), 112.3 (C), 113.4 (2 CH), 114.6 (C), 117.8 (C), 119.6 (CH), 124.5 (CH), 125.6 (CH), 126.2 (C), 127.5 (C), 130.8 (2 CH), 131.5 (CH), 132.4 (C), 142.7 (C), 144.7 (C), 156.3 (C), 161.7 (C=O), 163.5 (C=O), 164.8 (C=O), 183.4 (C=O) ppm. EI-MS: 504 (M$^+$, 15), 473 (68), 31 (100). Anal. Calcd. for $C_{27}H_{24}N_2O_8$ (504.49): C, 64.28; H, 4.80; N, 5.55; found: C, 64.42; H, 4.98; N, 5.72%.

dimethyl 1-(2-ethoxy-2-oxoacetyl)-5-(4-nitrophenyl)-7H-benzo[f]pyrrolo[1,2-d][1,4]diazepine-2,3-dicarboxylate (6i):

Yellow powder, mp 163-165˚C, 0.84 g, Yield 90%; FT-IR (KBr) (γ_{max}/cm^{-1}): 3556, 1742, 1727, 1697,

1589, 1487, 1296 cm^{-1}. ^1H NMR (500 MHz, $CDCl_3$): δ= 1.28 (3 H, t, ^3J = 7.4 Hz, CH_3), 3.75 (3 H, s, MeO), 3.87 (3 H, s, MeO), 4.26 (2 H, q, ^3J = 7.4 Hz, CH_2O), 7.08 (1 H, d, ^3J =7.6 Hz, CH), 7.15 (1 H, t, ^3J = 7.6 Hz, CH), 7.26 (1 H, s, CH), 7.37 (1 H, t, ^3J = 7.6 Hz, CH), 7.46 (1 H, d, ^3J = 7.6 Hz, CH), 7.67 (2 H, d, ^3J = 7.8 Hz, 2 CH), 7.87 (2 H, d, ^3J = 7.8 Hz, 2 CH), 12.35 (1 H, s, NH) ppm. ^{13}C NMR (125.6 MHz, $CDCl_3$): δ = 13.9 (CH_3), 51.6 (MeO), 52.4 (MeO), 62.5 (CH_2O), 110.7 (C), 112.3 (C), 113.8 (C), 114.2 (C), 120.4 (CH), 125.7 (CH), 126.3 (CH), 127.2 (CH), 128.3 (C), 129.5 (2 CH), 130.2 (2 CH), 131.6 (CH), 144.7 (C), 145.2 (C), 146.7 (C), 147.6 (C), 161.3 (C=O), 164.3 (C=O), 165.8 (C=O), 179.4 (C=O) ppm. EI-MS: 519 (M^+, 10), 488 (78), 31 (100). Anal. Calcd. for $C_{26}H_{21}N_3O_9$ (519.46): C, 60.12; H, 4.07; N, 8.09; found: C, 60.34; H, 4.22; N, 8.27%.

5-ethyl 2,3-dimethyl 1-(2-ethoxy-2-oxoacetyl)-7H-benzo[f]pyrrolo[1,2-d][1,4]diazepine-2,3,5-tricarboxylate (6j):

Pale yellow powder, mp 121-123˚C, 0.91 g, Yield 97%; FT-IR (KBr) (γ_{max}/cm^{-1}): 3548, 1742, 1729, 1695, 1587, 1486, 1295 cm^{-1}. ^1H NMR (500 MHz, $CDCl_3$): δ= 1.23 (3 H, t, ^3J = 7.4 Hz, CH_3), 1.34 (3 H, t, ^3J = 7.4 Hz, CH_3), 3.79 (3 H, s, MeO), 3.88 (3 H, s, MeO), 4.23 (2 H, q, ^3J = 7.4 Hz, CH_2O), 4.34 (2 H, q, ^3J = 7.4 Hz, CH_2O), 7.12 (1 H, t, ^3J =7.6 Hz, CH), 7.18 (1 H, d, ^3J = 7.6 Hz, CH), 7.42 (1 H, t, ^3J = 7.6 Hz, CH), 7.47 (1 H, d, ^3J = 7.6 Hz, CH), 7.56 (1 H, s, CH), 12.23 (1 H, s, NH) ppm. ^{13}C NMR (125.6 MHz, $CDCl_3$): δ = 13.8 (CH_3), 14.5 (Me), 51.6 (MeO), 52.6 (MeO), 61.5 (CH_2O), 62.6 (CH_2O), 103.5 (C), 113.6 (C), 117.3 (C), 119.5 (CH), 121.2 (CH), 123.7 (CH), 124.5 (C), 126.3 (CH), 128.3 (C), 131.2 (CH), 143.5 (C), 144.2 (C), 162.3 (C=O), 165.6 (C=O), 166.8 (C=O), 180.6 (C=O) ppm. EI-MS: 470 (M^+, 15), 439 (64), 425 (78), 31 (100). Anal. Calcd. for $C_{23}H_{22}N_2O_9$ (470.43): C, 58.72; H, 4.71; N, 5.95; found: C, 58.92; H, 4.89; N, 6.12%.

1,1-Diphenyl-2-picrylhydrazyl (DPPH) radical scavenging test

The DPPH radical scavenging experiment was utilized for investigation of some generated of pyrrolobenzodiazepines antioxidant ability such as **6a-6d** like the method reported by Shimada et. al.. [40] For obtaining to this object, various concentrations (200–1000 ppm) of pyrrolobenzodiazepines **6a-6d** were added to equal volume of DPPH methanolic solution (1 mmol/L). The mixture was stirred for 30 min at environmental temperature and putted in a dark room after this time and the absorbance of mixture was recorded at 517 nm. The schiff base of pyrrolobenzodiazepines **6a-6d** was replaced with standard type of methanol (3 mL). In this procedure, Butylated hydroxytoluene (BHT) and 2-tertbutylhydroquinone (TBHQ) are standard antioxidants. The percentage of inhibition for the radical of DPPH calculated by utilizing Yen and Duh [42] formula.

Study of reducing ability for synthesized pyrrolobenzodiazepines

The ability of iron (III) reducing by the pyrrolobenzodiazepines **6a-6d** was investigated utilizing Yildirim et al. method**.**[43] For this object, the samples (1 mL), potassium ferricyanide ($K_3Fe(CN)_6$; 2.5 mL, 10g/L) and buffer of phosphate (2.5 mL, 0.2 mol/L, pH 6.6) were combined together and maintained for 30 min at 50 ^oC. Then, trichloroacetic acid (2.5 mL, 10% w/v) was added to the previous solution and centrifuged for 10 min. Finally, the supernatant (2.5 mL), distilled water (2.5 mL) and $FeCl_3$ (0.5 mL, 1 g/L) mixed together and the absorbance of samples was measured at 700 nm. The higher absorbance of sample show higher reducing power of it. For accuracy of calculating, each measuring was carried out in three times. One way study of variance (ANOVA) that was used for data analyzing of compounds is running the SPSS software version 18.0 that proved difference of samples and control. Duncan multiple range experiments was employed for separation mean with the importance quantity of 95% ($P < 0.05$).

References

[1] Kalaria, P. N.; Karad, S. C.; Raval, D. K. *Eur. J. Med. Chem.* **2018**, *158*, 917–936.

[2] Desai, N.; Trivedi, A.; Pandit, U.; Dodiya, A.; Rao, V. K.; Desai, P. *Mini. Rev. Med. Chem.* **2016**, *16*, 1500–1526.

[3] Fouad, M. M.; El-Bendary, E. R.; Suddek, G. M.; Shehata, I. A.; El-Kerdawy, M. M. *Bioorg. Chem.* **2018**, *81*, 587–598.

[4] Martins, P.; Jesus, J.; Santos, S.; Raposo, L. R.; Roma-Rodrigues, C.; Baptista, P. V.; Fernandes, A. R. *Molecules* **2015**, *20*, 16852–16891

[5] Siddiqui, N.; Andalip Bawa, S.; Ali, R.; Afzal, O.; Akhtar, M. J.; Azad, B.; Kumar, R. *J. Pharm. Bioallied. Sci.* **2011**, *3*, 194–212.

[6] Sokolova, A. S.; Yarovaya, O. I.; Bormotov, N. I.; Shishkina, L. N.; Salakhutdinov, N. F. *Med. Chem. Comm.* **2018**, *9*, 1746–1753.

[7] Goel, A.; Agarwal, N.; Singh, F. V.; Sharon, A.; Tiwari, P.; Dixit, M.; Pratap, R.; Srivastava, A. K.;

Maulik, P. R.; Ram, V. J. *Bioorg. Med. Chem. Lett.* **2004**, *14*, 1089–1092.
[8] Amir, M.; Javed, S. A.; Kumar, H. *Indian. J. Pharm. Sci*. **2007**, *69*, 337–343.
[9] Li, W.; Zhao, S. J.; Gao, F.; Lv, Z. S.; Tu, J. Y.; Xu, Z. *Chemistry Select* **2018**, *3*, 10250–10254.
[10] Zhao, X.; Chaudhry, S. T.; Mei, J. **2017**, *121*, 133–171.
[11] Khattab, T. A.; Rehan, M. A. . *Egypt. J. Chem.* **2018**, *61*, 989–1018.
[12] Lamberth, C.; Dinges, J. Bioactive heterocyclic compound classes: agrochemicals. Wiley-VCH Verlag GmbH & Co, KGaA, **2012**.
[13] Khalilzadeh, M. A.; Yavari, I.; Hossaini, Z.; Sadeghifar, H. *Monatsh. Chem.* **2009**, *140*, 467–471.
[14] Khaleghi, F,; Din, L. B.; Jantan, I.; Yaacob, W. A.; Khalilzadeh, M. A. *Tetrahedron Lett.* **2011**, *52*, 7182-7184.
[15] Tietze, L. F.; Bsasche, C.; Gericke, K. M. Domino reactions in organic synthesis. Wiley-VCH, Weinheim, **2006**.
[16] Weber L, Illgen M, Almstetter M. *Synlett* **1999**, *3*, 366–374
[17] Herrera, R. P.; Marqués-López, E. Multicomponent reactions: concepts and applications for design and synthesis. Wiley, Hoboken **2015**.
[18] (a) Ali Maleki, *Ultrason. Sonochem*. **2018**, *40*, 460-464, (b) Ali Maleki Mahboubeh Rabbani Shirin Shahrokh, *Appl. Organometal. Chem.* **2015**, *29*, 809-814; (c) Ali Maleki Morteza Aghaei Nakisa Ghamari, *Appl. Organometal. Chem.* **2016**, *30*, 939-942; (d) Ali Maleki Elnaz Akhlaghi Reza Paydar, *Appl. Organometal. Chem*. **2016**, 30, 382-3386.
[19] (a) Ali Maleki Narges Nooraie Yeganeh, *Appl. Organometal. Chem.* **2017**, 31, e3814; (b) Ali Maleki, *Polycycl. Aromat. Compd.* **2018**, *38*, 402-409; (c) Ali Maleki, *RSC Adv.* **2014**, *4*, 64169; (d) Ali Maleki, *Tetrahedron Lett.* **2013**, *54*, 2055; (e) Ali Maleki *Tetrahedron* **2012**, *68*, 7827.
[20] (a) Mojtaba Rouhi, Mohsen Babamoradi, Zoleikha Hajizadeh, Ali Maleki, Sajjad Tabar Maleki *Optik* **2020**, *212*, 164721; (b) Ali Maleki, Parisa Ravaghi, Morteza Aghaei and Hamed Movahed, *Res. Chem. Intermed.* **2017**, *43*, 5485 (c) Ali Maleki, Hamed Movahed and Reza Paydar *RSC Adv.* **2016**, *6*, 13657-13665.
[21] J. Mantaj, P.J. Jackson, K.M. Rahman, D.E. Thurston, *Angew Chem. Int. Ed. Engl*. **2017**, *56*, 462e488.
[22] M.J. Flynn, F. Zammarchi, P.C. Tyrer, A.U. Akarca, N. Janghra, C.E. Britten, C.E. Havenith, J.N. Levy, A. Tiberghien, L.A. Masterson, C. Barry, F. D'Hooge, T. Marafioti, P.W. Parren, D.G. Williams, P.W. Howard, P.H. van Berkel, J.A. Hartley, *Mol. Cancer Ther*. **2016**, *15*, 2709e2721.
[23] M.S. Kung Sutherland, R.B. Walter, S.C. Jeffrey, P.J. Burke, C. Yu, H. Kostner, I. Stone, M.C. Ryan, D. Sussman, R.P. Lyon, W. Zeng, K.H. Harrington, K. Klussman, L. Westendorf, D. Meyer, I.D. Bernstein, P.D. Senter, D.R. Benjamin, J.G. Drachman, J. A. *McEarchern, Blood* **2013**, *122*, 1455e1463.
[24] M. Amirsoleimani, M. A. Khalilzadeh, D. Zareyee. *J. Mol. Struc.*, **2021**, *1225*, 129076.
[25] (a) M. Keyhaniyan, A. Shiri, H. Eshghi, A. Khojastehnezhad, *Applied Organometallic Chemistry*, **2018**, *32*, e4344; (b) Zohreh Ghadamyari, Ali Shiri, Amir Khojastehnezhad, Seyed Mohammad Seyedi *Appl Organometal Chem.* **2019**, e5091; (c) Marziyeh Rohaniyan, Abolghasem Davoodnia, S. Ali Beyramabadi, Amir Khojastehnezhad, *Appl Organometal Chem.* **2019**;e4881.
[26] (a) Mahdi Keyhaniyan Amir Khojastehnezhad Hossein Eshghi Ali Shiri *Applied Organometallic Chemistry*, **2017**, *35*, e6158; (b) Farzaneh Tajfirooz, Abolghasem Davoodnia, Mehdi Pordel, Mahmoud Ebrahimi, Amir Khojastehnezhad *Appl Organometal Chem.* **2017**;e3930; (c) Behrooz Maleki, Samaneh Barat Nam Chalakia , Samaneh Sedigh Ashrafia , Esmail Rezaee Sereshta , Farid Moeinpourb , Amir Khojastehnezhadc and Reza Tayebee *Appl Organometal Chem.* **2015**, *29*, 290-295
[27] I. E. Wachs. *Catal. Today*. 2005, 100, 79–94.
[28] Z. Guo, B. Liu, Q. Zhang, W. Deng, Y. Wang, Y. Yang. *Chem. Soc. Rev.*, 204, 43, 3480–3524.
[29] A. Dastan, A. Kulkarnia, B. Torok. *Green Chem.*, **2012**, *14*, 17–37.
[30] M. Jabłonska, R. Palkovits *Catal. Sci. Technol.*, **2016**, *6*, 49–72.
[31] J. Shi. *Chem. Rev.*, **2013**, *113*, 2139–2181.
[32] S. Lin-Bing, L. Xiao-Qin, Z. Hong-Cai. *Chem. Soc. Rev.*, **2015**, *44*, 5092–5147.
[33] Q. Zhang, K.D.V. Vigier, S. Royer, F. Jerome. Chem. Soc. Rev., 2012, 41, 7108–7146.
[34] E. Kalantari, M. A. Khalilzadeh, D. Zareyee, M. Shokouhimehr. *J. Mol. Struc.*, **2020**, *1218*, 128488.
[35] M. A. Khalilzadeh, S. Hosseini, A. S. Rad, R. A. Venditti. *J. Agric. Food Chem.*, **2021**, *68*, 8710-8719.
[36] U. Heiz, E.L. *J. Mater. Chem.*, **2004**, 14, 564–577.
[37] E. Rafiee, S. Eavani. *RSC Adv.*, **2016**, 6, 46433–46466.
[38] J.R. Copeland, I.A. Santillan, S.M. Schimming, J.L. Ewbank, C. Sievers. *J. Phys. Chem. C*, **2013**, 117, 21413–21425.
[39] L.D. Trizio, L. Manna. *Chem. Rev.*, **2016**, 116, 10852–10887.

[40] P. Xiaoyang, Y. Min-Quan, F. Xianzhi, Z. Nan, X. Yi-Jun. *Nanoscale*, **2013**, 5, 3601–3614.
[41] B.F.G. Johnson. *Top. Catal*. **2003**, 24,147−159.
[42] M.B. Gawande, P.S. Branco, K. Parghi, J.J. Shrikhande, R.K. Pandey, C.A.A. Ghumman, N. Bundaleski, O. Teodoro, R.V. Jayaram. *Catal. Sci. Technol*. **2011**, 1, 1653−1664.
[43] S. Brauch, S.S. van Berkel, W. Westermann. *Chem. Soc. Rev.,* **2013**, 42, 4948–
4962.
[44] H.Y. Cho, J.P. Morken. *Chem. Soc. Rev.,* **2014**, 43, 4368–4380.
[45] B. Eftekhari-Sis, M. Zirak, A. Akbari. *Chem. Rev.,* **2013**, 113, 2958–3043.
[46] K. Sambasivarao, C.S. Arjun, G. Deepti. *ACS Comb. Sci.,* **2015**, 17, 253–302.
[47] B.H. Rotstein, S. Zaretsky, V. Rai, A.K.Yudin. *Chem. Rev.,* **2014**, 114, 8323–8359.
[48] M.S. Singh, S. Chowdhury. *RSC Adv.,* **2012**, 2, 4547–4592.
[49] S. Laurent, D. Forge, M. Port, A. Roch, C. Robic, L. Vander Elst, R.N. Muller. *Chem. Rev.,* **2008**, 108, 2064–2110.
[50] A. Corma, H. Garcia. *Chem. Soc. Rev.,* **2008**, 37, 2096−2126.
[51] V. Polshettiwar, R. Luque, A. Fihri, H. Zhu, M. Bouhrara, J.M. Basset. *Chem. Rev.,* **2011**, 111, 3036−3075.
[52] R. Prasad, P. Singh. *Catal. Sci. Technol*., **2013**, 3, 3326−3334.
[53]Ali Maleki , Razieh Firouzi-Haji , Zoleikha Hajizadeh, *Int. J. Biol. Macromol*. **2018**, 116, 320-326.
[54] Zoleikha Hajizadeh, Ali Maleki *Mol. Catal.* **2018**, 460, 87-93
[55] Reza Eivazzadeh-Keihan, Fateme Radinekiyan, Ali Maleki, Milad Salimi Bani, Zoleikha Hajizadeh, Somayeh Asgharnasl *Int. J. Biol. Macromol*. **2019**, 140, 407-414
[56]Maleki, A.; Ghassemi, M.; Firouzi-Haji, R. *Pure Appl. Chem. 2018*, 90, 387–394.
[57]Somayeh Asgharnasl, Reza Eivazzadeh-Keihan, Fateme Radinekiyan, Ali Maleki *Int. J. Biol. Macromol.* **2020**, 144, 29-46.
[58] Nasrollahzadeh M, Maham M, Rostami-Vartooni A, Bagherzadeh M, Sajadi SM. *RSC Adv* **2015**;5:64769e80.
[59] (a) B. Halliwell, *Free Radical Res.* **1999**, *31*, 261–272; (b) F. Ahmadi, M. Kadivar, M. Shahedi, *Food Chem.* **2007**, *105*, 57–64.
[60] M. A. Babizhayev, A. I. Deyev, V. N. Yermakovea, I.V. Brikman, J. Bours, *Drugs R D* **2004**, *5*, 125–139.
[61] L. Liu, M. Meydani, *Nutr. Rev.* **2002**, *60*, 368–371.
[62] a) E. Ezzatzadeh, Z. S. Hossaini, *Natural Product Research,* **2019**, *33*, 1617-1623.
[63] Ezzatzadeh, E.; Hossaini, Z. S. *Natural Product Research*, **2020**, *34*, 923-929.
[64] a) E. Ezzatzadeh, Z. S. Hossaini, *Molecular Diversity*, **2019**, *24*, 81-91. b) M. Rajabi, Z. S. Hossaini, M. A. Khalilzadeh, Sh. Datta, M. Halder, Sh. A. Mousa, *Journal Photochemistry and Photobiology B: Biology*, **2015**, *148*, 66-72.
[65] a) Z. S. Hossaini, D. Zareyee, F. Sheikholeslami-Farahani, S. Vaseghi, and A. Zamani, *Heteroat. Chem*., **2017**, *28*, e21362 b) F. Rostami-charati, Z. S. Hossaini, D. Zareyee, S. Afrashteh and M. Hosseinzadeh *J. Heterocycl. Chem.*, **2017**, *54*, 1937-1942.
[66] a) F. Rostami-Charati, Z. S. Hossaini, R. Rostamian, A. Zamani, and M. Abdoli *Chem. Heterocycl. Compd.*, **2017**, *53*, 480-483, (b) S. Rezayati, F. Sheikholeslami-Farahani, Z. S. Hossaini, R. Hajinasiri, and S. Afshari Sharif Abad *Comb. Chem. High Throughput Screening*, 2016, 9, 720-727.
[67] (a) I. Yavari, M. Sabbaghan, and Z. S. Hossaini, *Synlett* **2008**, 1153-1154. (b) F. Tavakolinia, T. Baghipour, Z. S. Hossaini, D. Zareyee, and M. A. Khalilzadeh *Nucleic Acid Ther*., **2012**, *22*, 265-270.
[68] a) I. Yavari, S. Seyfi, Z. S. Hossaini, M. Sabbaghan, and F. Shirgahi-Talari, Monatshefte *für Chemie-Chemical Monthly*, **2008**, *139*, 1479-1482. (b) M. A. Khalilzadeh, Z. S. Hossaini, M. M. Baradarani, and A. Hasannia *Tetrahedron* **2010,** *66*, 8464-8467. (c) R. Hajinasiri, Z. S. Hossaini, and F. Rostami-Charati, *Heteroat. Chem.*, **2011**, *22*, 625-629.
[69] a) F. Rostami-Charati, Z. S. Hossaini, and M. R. Hosseini-Tabatabaei, *Phosphorus, Sulfur, and Silicon and the Related Elements*, **2011**, *186*, 1443-1448. (b) S. Rezayati, F. Sheikholeslami-Farahani, Z. S. Hossaini, and R. Hajinasiri, *Comb. Chem. High Throughput Screening*, **2016**, *19*, 720-727. (c) F. Rostami-Charati, Z. S. Hossaini, F. Sheikholeslami-Farahani, and Z. Aziz, *Comb. Chem. High Throughput Screening*, **2015**, *18*, 872-880.
[70] I. Yavari, M. Ghazanfarpour-Darjani, Z. S. Hossaini, M. Sabbaghan, and N. Hosseini, *Synlett* **2008**, *2008*, 889-891.

[71] I. Yavari, M. Nematpour, and Z. S. Hossaini *Monatshefte für Chemie-Chemical Monthly*, **2010**, *141*, 229-232.
[72] I. Yavari, Z. S. Hossaini, S. Souri, and S. Seyfi, *Mol. Divers.*, **2009**, *13*, 439.
[73] I. Yavari, Z. S. Hossaini, *Tetrahedron lett.*, **2006**, *47*, 4465-4468.
[74] Rajendran, S. P.; Sengodan, K. *Journal of Nanoscience*, **2017**, 17, 1-7.
[75] Y. Li, H. Zhang, Z. Guo, J. Han, X. Zhao, Q. Zhao, S. J. Kim, *Langmuir* **2008,** 24, 8351−8357.
[76] G. Tian, K. Pan, H. Fu, L. Jing, W. Zhou, *J. Hazard. Mater.***2009,** 166, 939−944.
[77] X. Yang, Y. Wang, L. Xu, X. Yu, Y. Guo, *J. Phys. Chem. C* **2008**, 112, 11481−11489.
[78] J. M. Hermann, J. Disdier, P. *J. Pichat, Phys. Chem.* **1986**, 90, 6028−6034.
[79] A. Sclafani, J. M. Hermann, *J. Photochem. Photobiol. A* **1998**, 113, 181−188.
[80] M. Sabbaghan, Z. Hossaini, *Comb. Chem. High T. Scr.* **2012**, 5(9), 745-748.